Erratum

Correction to "Quantitative Analysis of Magnetic Resonance Radio-Frequency Coils Based on Method of Moment"

Fa-Hsuan Lin, Shyh-Kang Jeng, Wei-Peng Kuan, and Jyh-Horng Chen

In the above paper,[1] the order of the author list was incorrect. The list should have read as follows: Fa-Hsuan Lin, Shyh-Kang Jeng, Wei-Peng Kuan, and Jyh-Horng Chen.

Manuscript received October 24, 1999.

F.-H. Lin, S.-K. Jeng, and J.-H. Chen are with the Department of Electrical Engineering, National Taiwan University, Taipei, Taiwan, R.O.C.

W.-P. Kuan is with the Department of Biotechnology, National Yang-Ming University, Taipei, Taiwan, R.O.C.

Publisher Item Identifier S 0018-9464(00)00774-3.

[1]J.-H. Chen, S.-K. Jeng, W.-P. Kuan, and F.-H. Lin, *IEEE Trans. Magn.*, vol. 35, pp. 2118–2127, May 1999.

Quantitative Analysis of Magnetic Resonance Radio-Frequency Coils Based on Method of Moment

Jyh-Horng Chen, *Member, IEEE*, Shyh-Kang Jeng, *Member, IEEE*, Fa-Hsuan Lin, and Wei-Peng Kuan

***Abstract*— To investigate both spectral and spatial domain characteristics of radio-frequency coils in magnetic resonance experiments, we have developed a new approach based on the method of moment. Instead of the conventional point-matching scheme, the loop testing function is used. Such a testing function decreases the complexity of computation and elevates the efficiency of simulation. With the proposed testing function incorporated with a pulse basis function based on coil geometry topology, performance of both surface coil and volume coil can be predicted with consistent results compared with experiment data.**

***Index Terms*—Magnetic resonance, method of moment, MRI, radio-frequency coil.**

I. Introduction

NUCLEAR magnetic resonance (NMR) experiments, including some medical or biological applications, such as magnetic resonance imaging (MRI) and magnetic resonance spectroscopy (MRS), all need radio-frequency (RF) coils for signal excitation and acquisition. To get perfect results from these experiments, a homogeneous time-harmonic magnetic field at the transverse plane, the B1 field, oscillating at Larmor frequency of the scanner is desired for optimal performance. During development of RF coils, we need to evaluate the magnetic field quantitatively from current distribution on the coil due to its geometry and excitation/acquisition scheme for feasible design.

Traditionally, the RF coil simulation is implemented by a dc model based on Biot–Savart's law [1]. This model can process essentially all meshes of RF coils with fast computation, but it needs the assumed current distribution on the coil as the basis of analysis, while the current distribution is generally not so intuitively available in either high field magnetic resonance scanners or complicated coil geometry.

Due to this constraint, the dc model is not capable of coil performance prediction with satisfactory results. In addition, mutual impedance effect which is important in phased array coils [2] design and other coil meshes, such as mutual impedance of birdcage coils [3], end rings, and legs, cannot be evaluated via this traditional method either. Thus ac models with tolerable computation speed and physical insights are necessary for further high performance RF coil design.

Manuscript received February 15, 1997; revised February 12, 1998.

J.-H. Chen, S.-K. Jeng, and F.-H. Lin are with the Department of Electrical Engineering, National Taiwan University, Taipei, Taiwan (e-mail: chen@me.ee.ntu.edu.tw; skjeng@ew.ee.ntu.edu.tw).

W.-P. Kuan is with the Department of Biotechnology, National Yang-Ming University, Taipei, Taiwan, R.O.C.

Publisher Item Identifier S 0018-9464(99)02789-2.

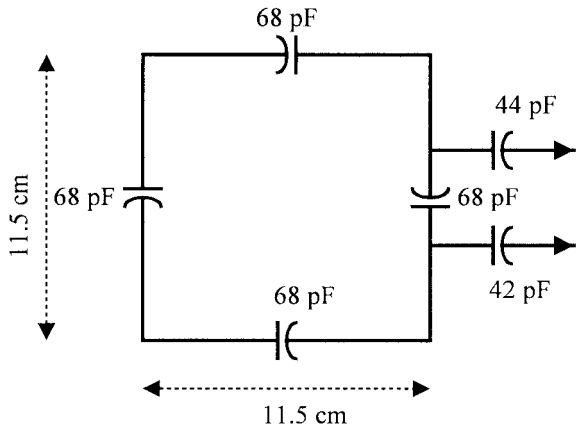

Fig. 1. Mechanical and electric parameters of square surface coil. The width of the conductor strips consisting the coil is 0.5 cm.

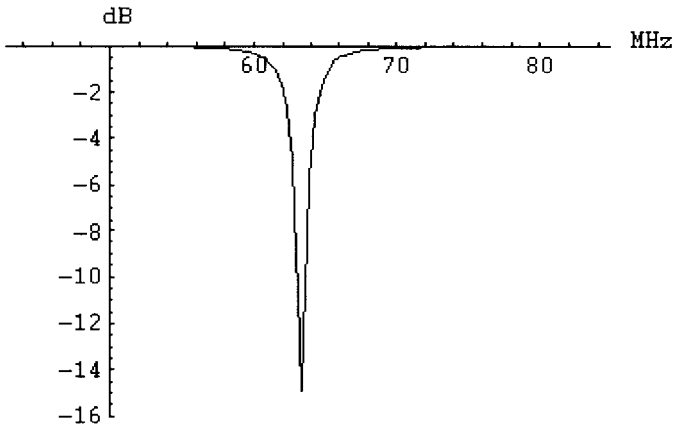

Fig. 2. Simulated frequency response of single square surface coil by method of moment.

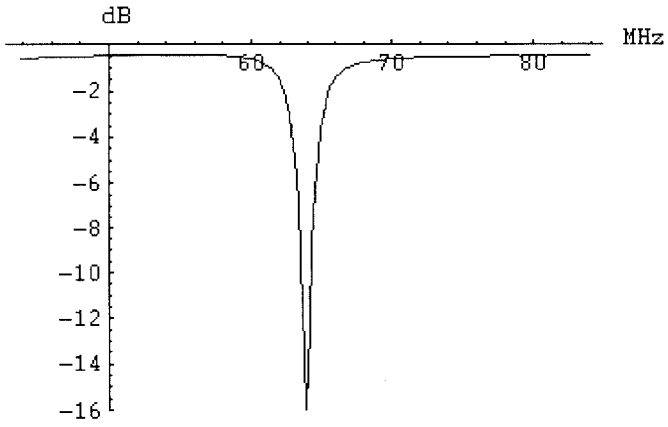

Fig. 3. Frequency response of single square surface coil measured from network analyzer.

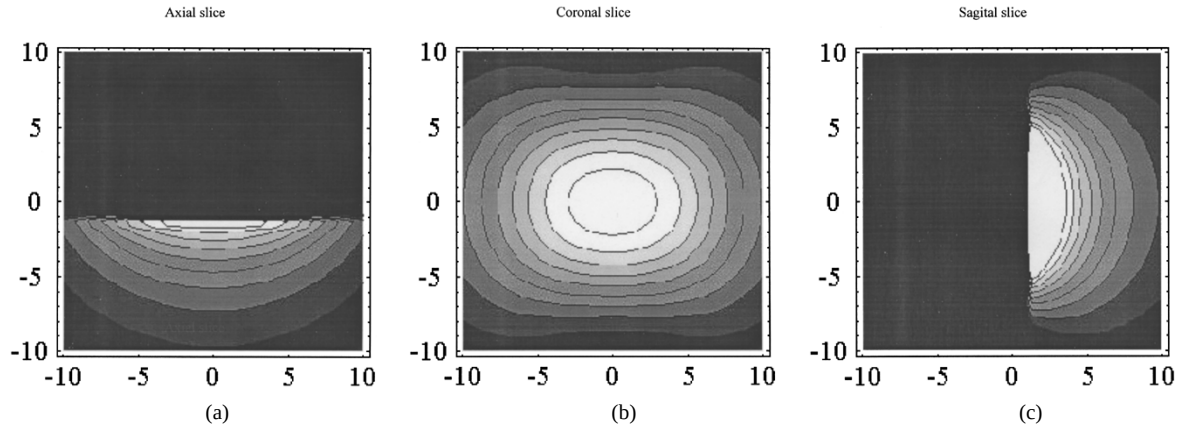

Fig. 4. Simulated phantom images of three directional slices. All images are normalized between zero and one. Contours are ten gray levels of iso separation. Images slices are named according to the patient position of head-first-in and supine. Axial $(x–y$ plane) and sagital $(x–z)$ plane slices are aligned with iso center of the scanner. Coronal $(y–z$ plane) slice image is 3 cm below the surface coil.

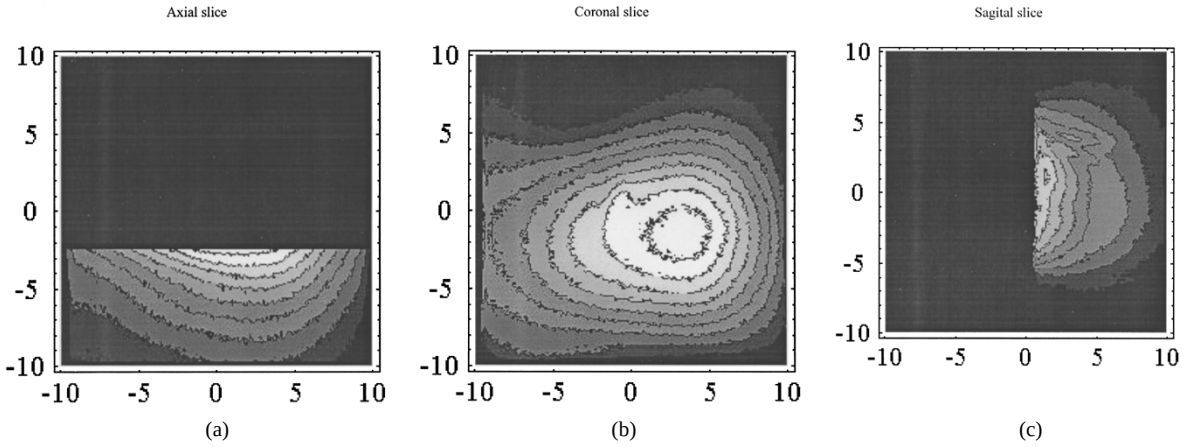

Fig. 5. Phantom images of three directional slices from experiment.

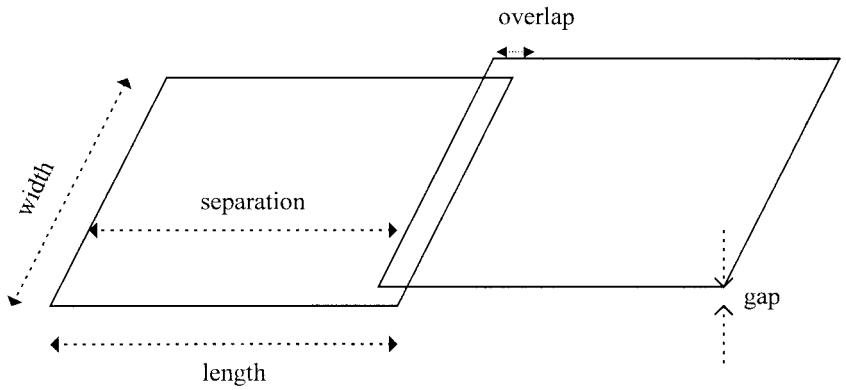

Fig. 6. The mesh of two-port phased array coil. Each of the surface coil has identical geometry as described in Fig. 1.

Lots of numerical simulation approaches, such as the finite-difference-time-domain method [4] and the finite element method [5], are proposed for sophisticated RF coil performance calculation, but these approaches generally suffer from high load and high complexity of computation. This drawback stumbles the availability of quantitative analysis of RF coils to wide range applications.

Here we propose a new simulation approach based on method of moment [6]. Instead of conventional pulse testing function or point matching schemes [7], [8], we use the loop as a testing function incorporated with appropriate basis according to the coil geometry. In addition to the capability of simulating both spectral and spatial domain data from coil geometry and input voltage only, the adoption of loop testing

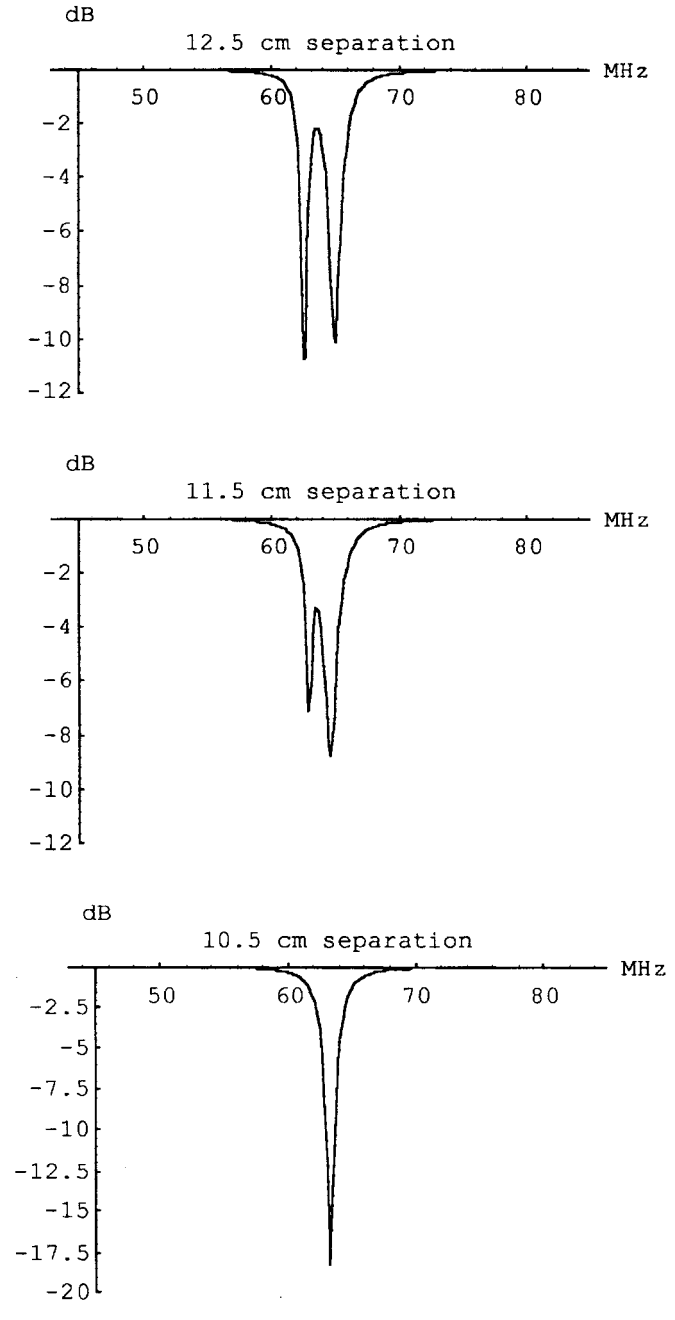

Fig. 7. Simulated frequency response of two-port phased array coil by method of moment.

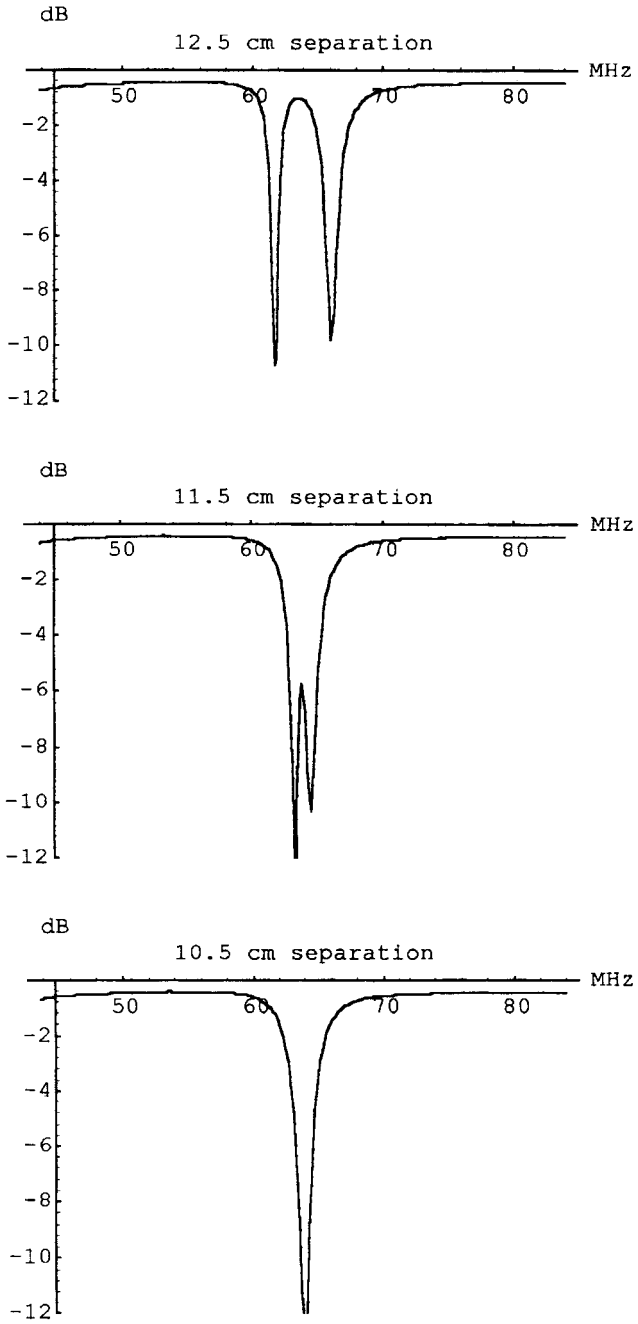

Fig. 8. Frequency response of two-port phased coil measured from network analyzer.

function decreases the computation complexity as well. This method is not only an ac model which takes time harmonic electromagnetic field properties into consideration without assuming current distribution on the coil, but it also embeds physical meaning about RF coil electrical properties. It needs no high load computation either. And with the aid of this method, we expect to quantify RF coil characteristics and provide us with insights for further RF coil designing.

II. Simulation Algorithm

Here we apply the theory of reciprocity [9] to simulate the characteristics of both transmission coils and reception coils. All analyses are based on the viewpoints of transmission coils.

As in a conventional scattering problem, here we solve the unknown current distribution on the RF coil by decomposing the problem into two parts. One is the impressed voltage regarded as the incident electric field source. And the other part is the scattered field due to an RF coil which functions as an object of scattering. With the assumption that the RF coil is made of perfect electric conductor, and by applying the boundary condition on tangential electric field, an integral equation can be expressed as

$$\vec{E}_i^{\text{tangential}} = jw\vec{A}(\boldsymbol{J}) + \nabla\Phi(\sigma) \tag{1}$$

where $\boldsymbol{A}$ is the free space magnetic vector potential and Φ is the free space electric scalar potential. $\boldsymbol{J}$ and σ are the

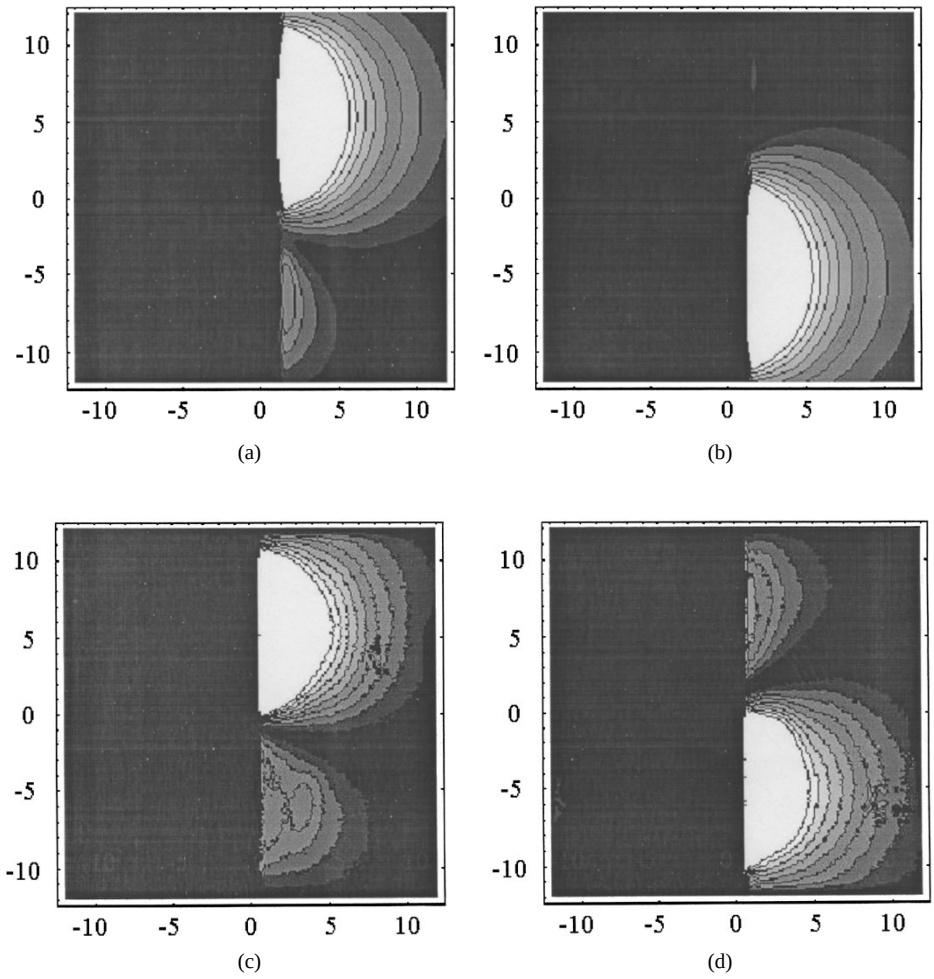

Fig. 9. Sagital slice images at two ports of the phased array coil from simulation and experiment. (a) Simulation of port 1, (b) simulation of port 2, (c) experiment image of port 1, and (d) experiment image of port 2.

current source and charge source induced on the surface of the coil, respectively, and the Larmor frequency of scanner is now embedded in the wave number k. To link the charge source and current source together, we use conservation of charge

$$\sigma(\overline{r}) = -\frac{\nabla \cdot \overline{J}(\overline{r})}{jw}. \tag{2}$$

If the conductor strip of the coil is quite thin and narrow enough, the volume source integral can be replaced by surface integral or line integral.

To solve electric field integral (1) by method of moment, loop testing functions are utilized. The loop function is a unit-intensity pulse along a loop on the coil. A loop is any closed logical route on the topology of the circuit. The loop function can be defined as

$$\boldsymbol{P}_n(\boldsymbol{r}) = \begin{cases} 1 \cdot \hat{c}, & \text{for } \boldsymbol{r} \text{ on the coil strip, } \hat{c} \text{ is the unit vecor along the tangential direction of the coil strip} \\ 0, & \text{otherwise.} \end{cases} \tag{3}$$

The divergence of a loop function is

$$\nabla \cdot \boldsymbol{P}_n(\boldsymbol{r}) = \begin{cases} \pm\delta(\boldsymbol{r}) & \text{at the boundary of the loop} \\ 0 & \text{otherwise.} \end{cases} \tag{4}$$

Current distribution on the RF coil with appropriate bases can be expressed as

$$\boldsymbol{J} = \sum_{n=1}^{N} I_n \cdot \boldsymbol{B}_n(\boldsymbol{r}) \tag{5}$$

where $\boldsymbol{B}_n$ is one of the current bases, and I_n is the corresponding coefficient. As in dc model, an RF coil is decomposed into linear segments, and each segment is a basis.

Then we define the inner product of two functions as the following:

$$\langle \boldsymbol{f} \cdot \boldsymbol{g} \rangle = \int_L \overline{f} \cdot \overline{g}\, ds. \tag{6}$$

The line integral is along the direction of testing loop on the coil.

We then apply the inner product operation on both sides of (1), and we use loop pulse function as testing function. This leads to

$$\langle \overline{E_i}, \overline{P_n}(\overline{r}) \rangle = jw \langle \overline{A}, \overline{P_n}(\overline{r}) \rangle + \langle \nabla\Phi, \overline{P_n}(\overline{r}) \rangle. \tag{7}$$

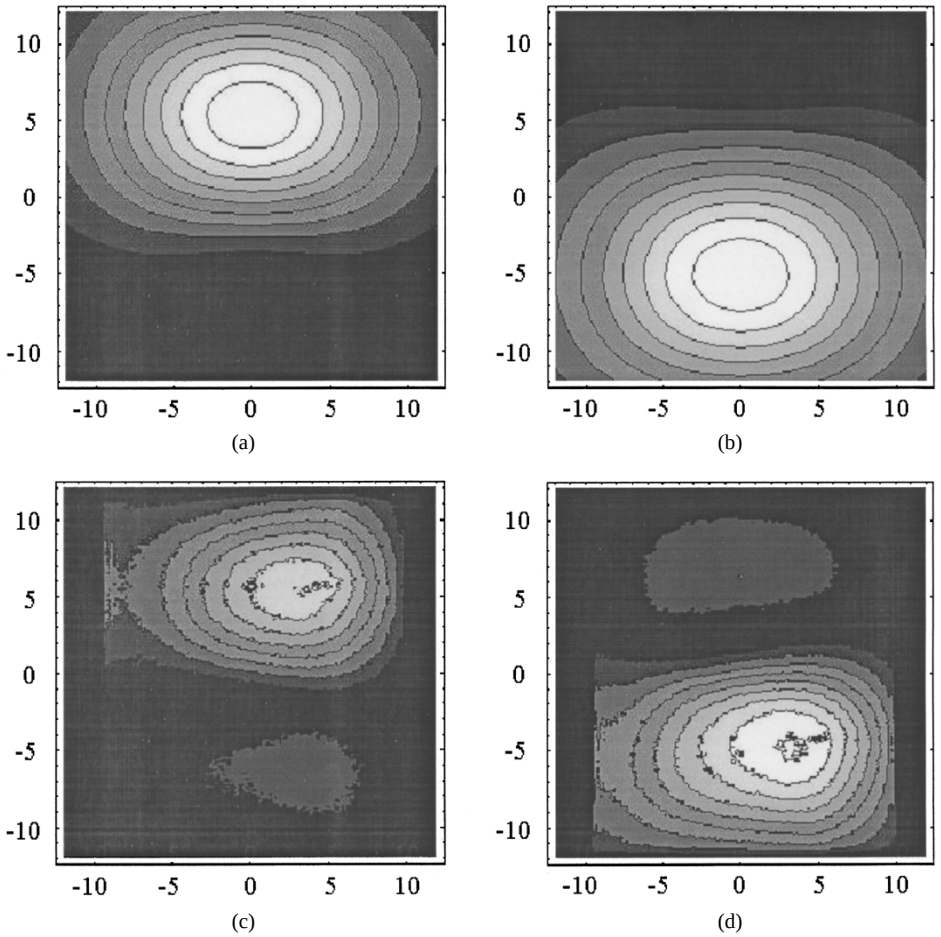

Fig. 10. Coronal slice images at two ports of the phased array coil from simulation and experiment. (a) Simulation (port 1), (b) simulation (port 2), (c) experiment (port 1), and (d) experiment (port 2).

To simplify the last term on the right-hand side of the equation above, we apply

$$\langle \nabla\Phi, \overline{P_n}(\bar{r})\rangle = \int_L \nabla\Phi \cdot \overline{P_n}(\bar{r})\, dl = \int_L (\nabla\cdot\Phi\overline{p_n}(\bar{r}) - \Phi\nabla\cdot\overline{p_n}(\bar{r}))\, dl = 0. \quad (8)$$

We see that the benefit of loop testing function is that it eliminates the scalar potential term in inner product, and thus simplifies the calculation.

The testing results of E_i and A are

$$\left\langle \left| \begin{matrix} \boldsymbol{A} \\ \boldsymbol{E}_i \end{matrix} \right|, \boldsymbol{P}_n(\boldsymbol{r}) \right\rangle = \int_L \left| \begin{matrix} \boldsymbol{A} \\ \boldsymbol{E}_i \end{matrix} \right| \cdot d\boldsymbol{l} \quad (9)$$

which can be further expanded with free space Green's function and solved by numerical integration, while the incident electric field term can be written as

$$\langle \vec{E_i}, \vec{P_n}(\vec{r})\rangle = V. \quad (10)$$

This inner-product represents the voltage drop across the testing loop due to the impressed voltage source. Formula (10) can be explained as the "observed" voltage drop V as we measure along the closed loop for the induced voltage, self or mutual induced voltages are included, generated by a unit-intensity pulse current P_n.

Since we have decomposed the current on the coil into linear combination of basis functions, we can formulate this problem into a matrix form, which enables the utilization of a computer for highly efficient computation.

The matrix equation is of the following form

$$[Z]\cdot[I] = [V] \quad (11)$$

where $[Z]$ is the impedance matrix, which is derived from the inner product (9)

$$Z_{mn} = jw \int_{\text{loop}\, m} \overline{A_n} \cdot \hat{c}_m dl_m \quad (12)$$

$\hat{c}_m$ is the unit vector along the loop m.

The entry Z_{mn} in the impedance matrix represents the voltage drop along loop m for a unit-intensity current on basis n. Since impedance matrix is a nondiagonal matrix, it includes the mutual impedance effects which are neglected in the dc simulation approaches.

During the calculation of mutual inductance, if the size of each conductor strip is negligible compared to the space between different strips, then the volume integral on the calculation of vector potential can be simplified as a line

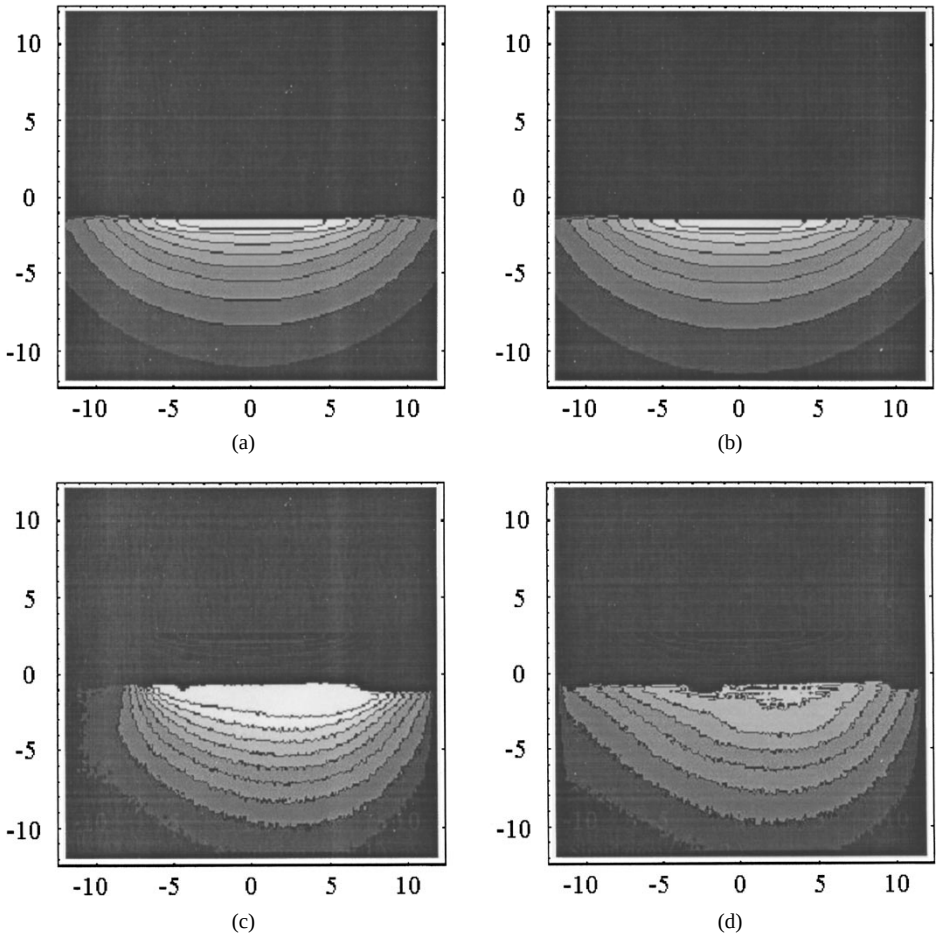

Fig. 11. Axial slice images at two ports of the phased array coil from simulation and experiment. (a) Simulation (port 1), (b) simulation (port 2), (c) experiment (port 1), and (d) experiment (port 2).

integral as following:

$$\overline{A_n} = \frac{\mu}{4\pi} \int_1 \frac{e^{-jk|\overline{r_m}-\overline{r_n}|}}{|\overline{r_m}-\overline{r_n}|} \cdot \hat{c}_n \, dl_n \tag{13}$$

where $\hat{c}_n$ is the unit vector along source basis n.

To simplify the calculation, we decompose the mesh of coil into linear combination of straight conductors. Such a combination is to approximate the real curved RF coil.

To avoid the singularity of the self-impedance, which comes from that we take current as a linear source, the finite width of coil strip must be taken into consideration. And the integration over source region is

$$\overline{A_n} = \frac{\mu}{4\pi} \int_{w_n} \int_{l_n} \frac{e^{-jk|\overline{r_m}-\overline{r_n}|}}{w_n \cdot |\overline{r_m}-\overline{r_n}|} \cdot \hat{c}_n \, dl_n \, dw_n \tag{14}$$

where $\hat{c}_n$ is the unit vector along source basis n.

In addition to the self/mutual impedance entries, the connection between bases must be incorporated to satisfy Kirchhoff current law (KCL) at nodes of RF coil. For a RF of N nodes and B branches, there should be $N-1$ KCL equations and $B-N+1$ independent loop testing function for current computation.

With the calculated complex current, frequency response of the RF coil is available. Magnetic field map can be acquired via Maxwell equations easily as well.

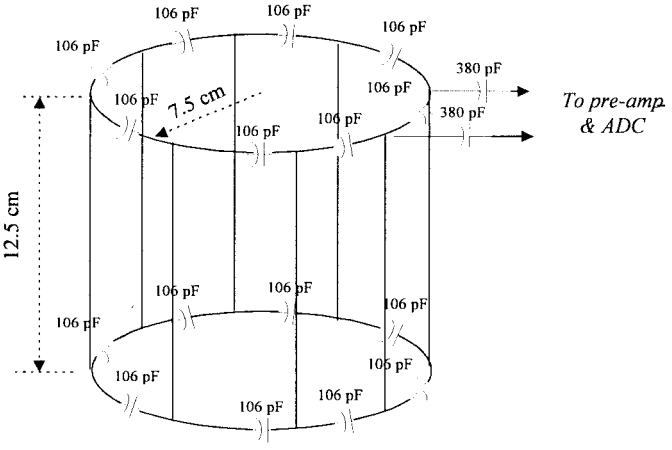

Fig. 12. Mechanical and electric parameters of eight-port high-pass knee-sized birdcage coil. The width of the conductor strips consisting the coil is 1.5 cm.

III. Methods and Material

To simplify the multiple integration in impedance matrix entries, the free space Green's function is approximated by the first four terms of its Taylor expansion. We implemented the simulation on a Sparc 20 workstation. The program is

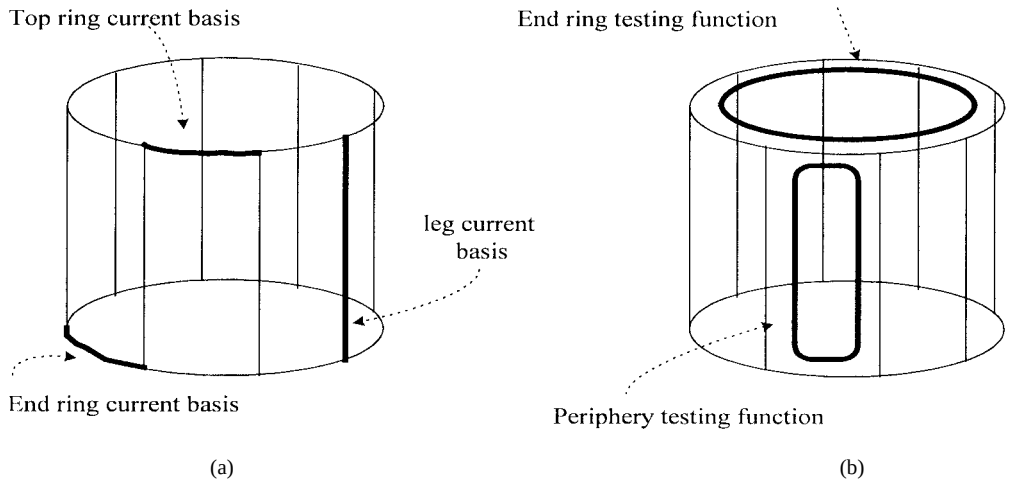

Fig. 13. Current basis and testing function for simulating eight-port birdcage coil. (a) Basis function. (b) Testing function.

written in ANSI C language. To evaluate the integral during calculation, Gaussian quadrature integration is utilized.

Here we simulate our cases for a 1.5 Tesla MR scanner, in which the Larmor frequency is about 64 MHz. All coils to be simulated are tuned to 64 MHz. MR images are acquired from GE Signa 1.5 Tesla scanner. While the frequency response of the coils are measured by Hewlett Packard 8751A Network Analyzer.

IV. Results

Here we demonstrate three cases for verification. The first one is a single square surface coil and the second one is a simple phased array coil consisting of two plane square surface coils. The third is a volume birdcage coil. Simulation results and corresponding experiment data are both included.

A. Single Square Surface Coil

The geometrical dimension and the electric components on the surface coil to be simulated and tested are both depicted in Fig. 1. Here loop function is adopted as both testing and basis function.

The frequency responses of the coils from simulation and from network analyzer are depicted in Figs. 2 and 3. We can see that there is a good match between simulation results and experiment data.

After spectral domain verification, we would like to extend our test on spatial domain characteristics. Phantom composed of saline is imaged for B_1 distribution. Simulation results are depicted in Fig. 4 for three directional slices. They are axial, sagital, and coronal slice, respectively. At the same time, we also show the B_1 distribution from experiment in Fig. 5 for comparison.

B. Two-Port Phased Array Coil Composed of Square Surface Coil

Besides single surface coil, multiple coil system is simulated, too. We choose a two-square-surface coil system to verify the validity of mutual inductance effects by our algorithm. Each of the surface coils is identical to the one described above. Layout and spatial coordinates of the two-port phased array coil is shown in Fig. 6. Testing functions for simulating this array system are two distinct loops along two surface coils, and basis functions are identical to testing functions. The simulated spectrums at three different separate distances are shown in Fig. 7. Frequency responses measured from network analyzer are shown in Fig. 8.

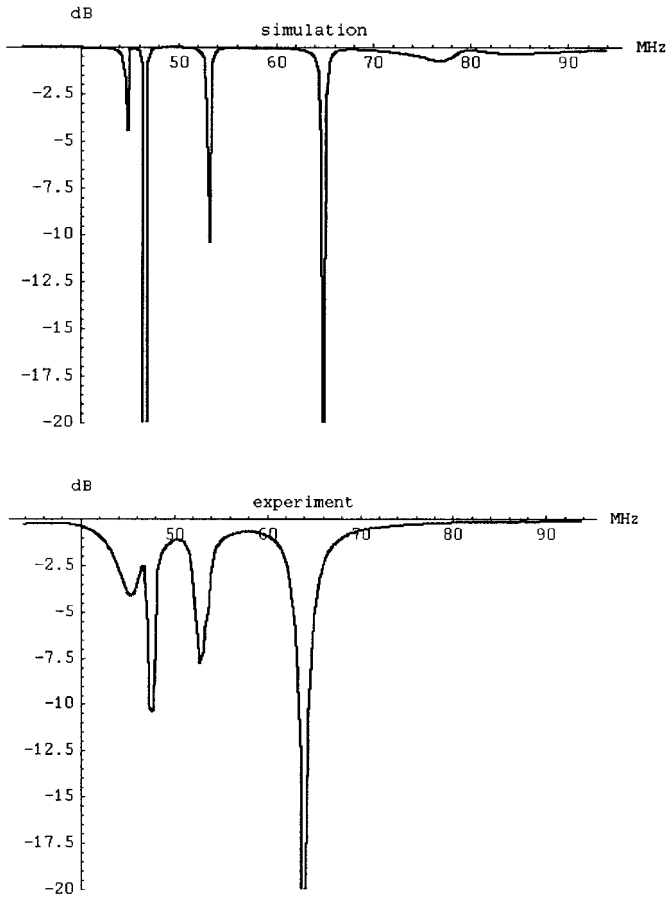

Fig. 14. Frequency response from simulation based on proposed algorithm and experiment.

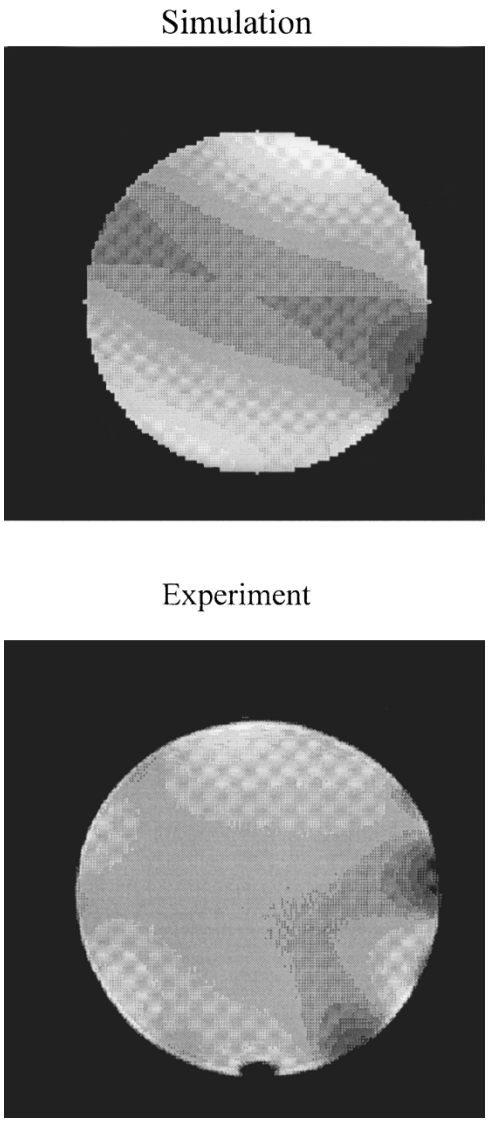

Fig. 15. Axial slice phantom image from simulation based on proposed algorithm and experiment.

Since we tuned the position of this two-surface coil system resonating at Larmor frequency, images are available now. The results from both simulation and experiments for different imaging slices are shown in Figs. 9–11.

C. Eight-Port Birdcage Coil

Birdcage coil is proposed for its homogeneous transverse magnetic field distribution compared to traditional volume coil. A birdcage coil consists of two end rings and several "legs" connected between end rings. An eight-port high-pass birdcage coil mesh with its mechanical and electrical specification is shown in Fig. 12. To use our proposed approach, 15 KCL equation and nine distinct testing loops must be incorporated together. KCL equations come from 16 nodes of the birdcage, while nine testing loops are eight periphery loops and one end-ring loop. Each segment between either two nodes is a current basis. Basis function and testing functions are depicted in Fig. 13.

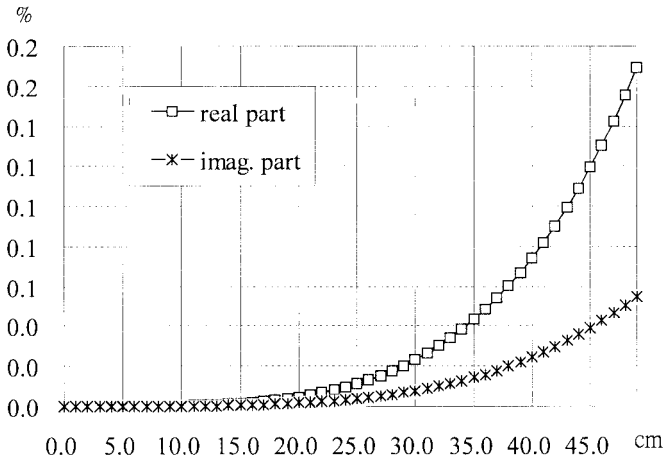

Fig. 16. Error plot for 1.5 Tesla MR scanner system. Error is defined as percentage deviation from sum of free space Green's function at different abscissas replaced by its first four terms of Taylor expansion. When the separation of coil strips is within 50 cm, this error is negligible in 1.5 Tesla scanner, which corresponds to operating frequency of 64 MHz.

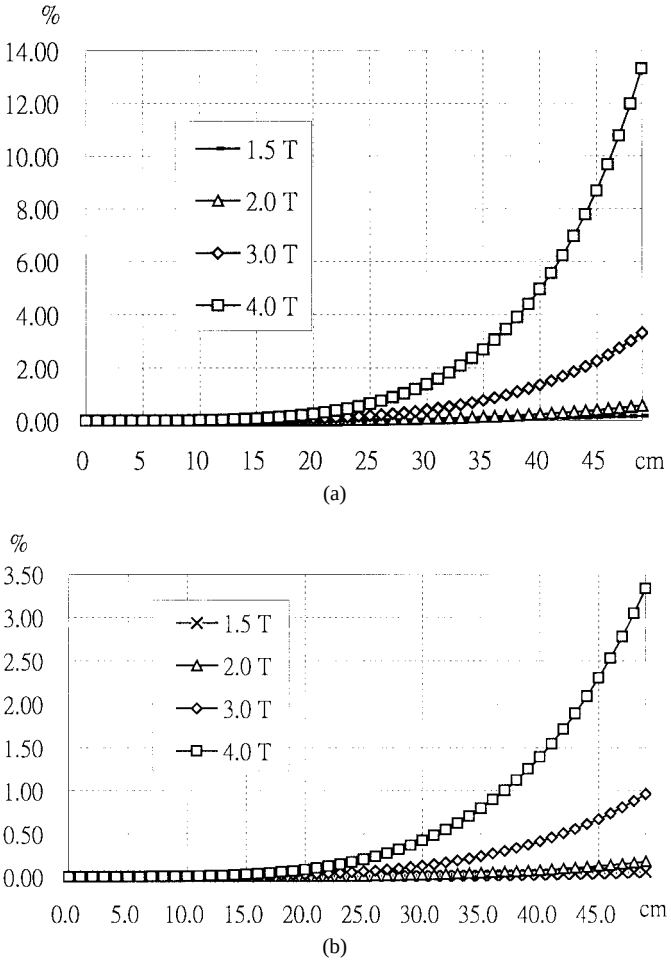

Fig. 17. (a) Real part error of approximation of free space Green's function by its first four Taylor series at scanners of different main field strength. (b) Imaginary part error of approximating free space Green's function by its first four terms in the Taylor series at scanners of different main field strength.

The frequency response of the birdcage coil is shown in Fig. 14, which includes both simulation results and experiment data from network analyzer. Fig. 15 demonstrates the B_1 field map from simulation and experiment.

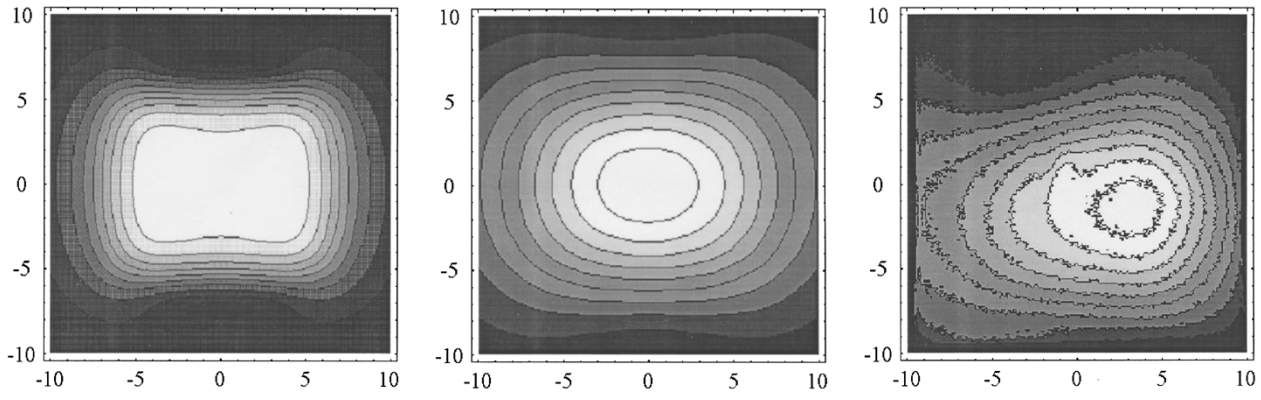

Fig. 18. (a) Comparison of coronal slice image of single square surface coil. The coronal slice is 3 cm below the coil plane. We can see that dc model predicts worse than ac model, because in dc model we have no idea about the appropriate current intensity on the coil due to coil geometry and electric component. Ac models can calculate current distribution directly from geometrical specification and component value, and thus appropriate current intensity incorporated with time-harmonic electromagnetic wave properties is available. (b) Comparison of axial slice image of eight-port high-pass birdcage coil. By proposed method, an oblique homogeneous transverse magnetic field is shown, which is consistent with the experiment result. While dc model cannot predict such performance, it overestimates the homogeneous region of the transverse magnetic region.

V. Discussion

Both spectral and spatial domain simulated characteristics of RF coils are consistent with experiment data. This is true for both surface and volume coils. Contrast to the conventional dc approach, we need input coil geometry and electric component on the RF coil, which can be measured with high precision, for evaluation of complex current distribution and further frequency response or transverse magnetic field mapping. Calculation of complex current includes self-impedance and mutual impedance between segments of the coil.

We use the first four terms of Taylor expansion on free space green's function for calculation of impedance entries. This approximation will introduce some error, which is shown in Fig. 16. The error from such approximation is less than 1.0% for separation of conductor strip within 50 cm in 1.5 Tesla system. For most clinical torso-bore applications, such a distance between coil strips is almost the maximal separation. Fig. 17 shows the error at MR scanners of different field strength. We see that even in a 4.0 Tesla scanner such an approximation introduces no severe deviation.

The phantom for imaging is equivalent to a resistance in simulation according to the literature [10]. Such a resistance derives from both dielectric loss and inductive loss. Some mismatch of frequency response of surface coil simulation may come from charge accumulation at corners of RF coil, which cannot be evaluated by loop basis function. Further decomposition of basis function can take this effect into evaluation.

Compared with traditional dc method, we show the simulation results from method of moment in Fig. 18. No matter surface or volume coil, the proposed model predicts closer to real cases. In Fig. 19, we also show the leg current distribution of the birdcage. Theoretically, current distribution at legs of birdcage with sinusoidal pattern of only one cycle produces the most homogeneous transverse magnetic field. From simulation, we can observe such a current distribution and assure the correct mode of the designed birdcage coil.

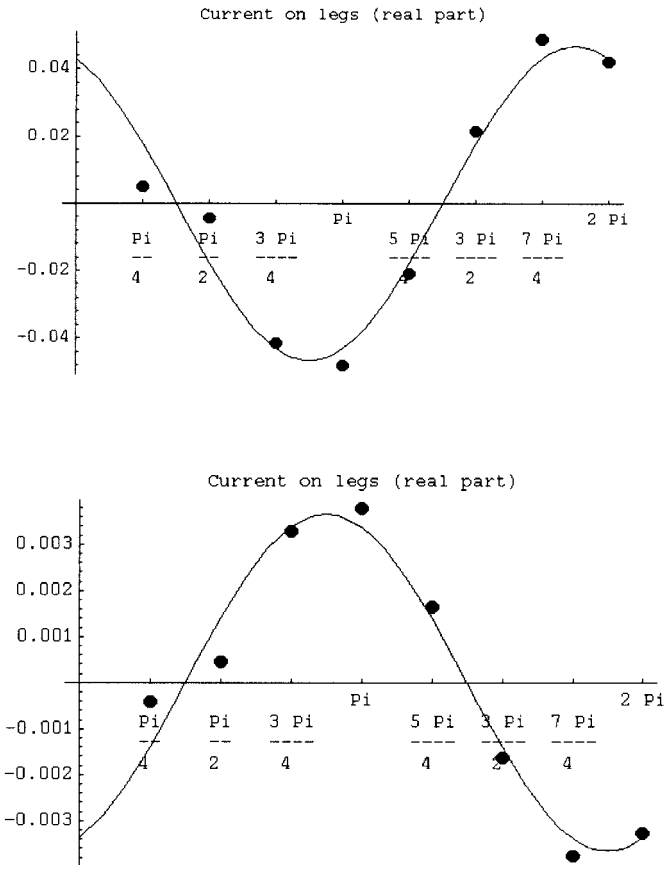

Fig. 19. Current distribution on legs of eight-port high-pass birdcage coil. This current distribution is fit for sinusoidal pattern of one cycle with satisfactory match.

VI. Conclusion

We have proposed a new simulation approach, which evaluates both spectral and spatial characteristics of MR RF coils from coil geometry definition. Without the presumed current, this model calculates complex current distribution on

RF coils automatically. Spectral and spatial data are then generated from the calculated currents. Instead of tedious and complicated computation, this approach embeds both high-efficiency computation and clear physical insight at the same time. Experiments are performed to verify the proposed simulation algorithm with satisfactory match. With the aids of this approach, RF coil quantitative investigations can be made for all applications.

REFERENCES

[1] W. T. Sobol, "Dedicated coils in magnetic resonance imaging," *Rev. Magn. Reson. Med.*, vol. 1, no. 2, pp. 181–224, 1986.

[2] P. B. Roemer, W. A. Edelstein, C. E. Hayes, S. P. Souza, and O. M. Mueller, "The NMR phased array," *Magn. Reson. Med.*, vol. 16, no. 2, pp. 192–225, Nov. 1990.

[3] C. E. Hayes, W. A. Edelstein, J. F. Schenck, O. M. Mueller, and M. Eash, "An efficient highly homogeneous radio frequency coil for whole-body NMR imaging at 1.5 T," *J. Magn. Reson.*, vol. 63, p. 622, July 1985.

[4] W. L. Ko, "Analyzes of RF coils in MRI by FD-TD," in *Proc. Annu. Conf. Eng. Med. Biology*, Orlando, FL, 1991, vol. 13, pt. 1, pp. 85–86.

[5] L. S. Petropoulos, E. M. Haacke, R. W. Brown, and E. Boerner, "Predicting RF field penetration in heterogeneous bodies using a 3-D finite element approach: Preliminary results," *Magn. Reson. Med.*, vol. 30, no. 3, pp. 366–372, Sept. 1993.

[6] R. F. Harrington, *Field Computation by Moment Methods*. New York: Macmillan, 1968.

[7] H. Tsuboi, H. Tanaka, and T. Misaki, "Electromagnetic field analysis of RF antenna for MRI," *IEEE Trans. Magn.*, vol. 24, pp. 2591–2593, Nov. 1988.

[8] M. Fujita, M. Higuchi, H. Tsuboi, H. Tanaka, and T. Misaki, "Design of the RF antenna for MRI," *IEEE Trans. Magn.*, vol. 26, pp. 901–904, Mar. 1990.

[9] D. I. Hoult and R. E. Richard, "The signal-to-noise ratio of the nuclear magnetic resonance experiment," *J. Magn. Reson.*, vol. 24, pp. 71–85, Jan. 1976.

[10] D. G. Gadian and F. N. H. Robinson, "Radio frequency losses in NMR experiments on electrically conducting samples," *J. Magn. Reson.*, vol. 34, pp. 449–455, May 1979.

Jyh-Horng Chen (S'89–M'91) was born in 1960. He received the B.S. degree from the Department of Electrical Engineering, National Taiwan University (NTUEE), Taipei, Taiwan, in 1982, the M.S. degree in biomedical engineering from National Yang Ming Medical College, Taipei, Taiwan, and the Ph.D. degree in bioengineering from University of California, Berkeley and University of California, San Francisco.

He joined the faculty of NTUEE as an Associate Professor in 1991. His research interests include medical informatics, magnetic resonance imaging, and man–machine interface for disables.

Dr. Chen is a member of SMRM and AAPM.

Shyh-Kang Jeng (M'87) was born in 1957. He received the B.S.E.E. and Ph.D. degrees from National Taiwan University, Taipei, Taiwan, R.O.C., in 1979 and 1983, respectively.

In 1981 he joined the faculty of the Department of Electrical Engineering, National Taiwan University, where he is now a Professor. From 1984 to 1985 he was an electronic data processing officer and an instructor on information system analysis and design at the National Defense Management College, Chung- Ho, Taiwan, R.O.C. From September 1985 to August 1986 and in the summer of 1988 he was a Visiting Research Associate Professor at the University of Illinois, Urbana. His current interest is in applying advanced computer techniques to electromagnetic field problems.

Fa-Hsuan Lin was born in 1972. He received the B.S.E.E. and M.S. degrees from National Taiwan University, Taipei, Taiwan, R.O.C., in 1994 and 1996, respectively. Currently he is working towards the Ph.D. degree in the Medical Engineering Medical Physics program at Harvard University-Massachusets Institute of Technology (MIT), Division of Health Science and Technology, and the Department of Electrical Engineering and Computer Science, MIT, Cambridge, MA.

His current research interests are signal processing, brain functions, and magnetic resonance imaging.

Wei-Peng Kuan was born in 1957. He received the B.S. degree from the Department of Nuclear Science, National Tsing Hua University, Hsin Chu, Taiwan, in 1980, the M.S. degree from the Department of Nuclear Engineering, North Carolina University, in 1984, and the Ph.D. degree from the Department of Nuclear Radiology, University of Florida, Gainesville, in 1989.

He joined the faculty of Magnetic Resonance Laboratory at Massachusetts's General Hospital, Boston, as an Associate Study Fellow in 1989. In 1990, he became an Associate Professor in the Department of Biotechnology, National Yang-Ming University, Taipei, Taiwan. His interest is in radiological medicine, MRI coils, and MRS.